JOURNAL OF PROPULSION AND POWER
Vol. 11, No. 2, March–April 1995

Ignition and Combustion Performance of Scramjet Combustors with Fuel Injection Struts

Goro Masuya,* Tomoyuki Komuro,† and Atsuo Murakami‡
National Aerospace Laboratory, Kakuda, Miyagi 981-15, Japan
Noboru Shinozaki§ and Akihiro Nakamura§
Nissan Motor Co., Ltd., Kawagoe, Saitama 350, Japan
and
Motohide Murayama¶ and Katsura Ohwaki**
Ishikawajima–Harima Heavy Industries, Tanashi, Tokyo 188, Japan

Ignition and combustion performance of a scramjet combustor with a fuel injection strut was experimentally investigated with Mach 2.5 vitiated air. Five strut models with different leading-edge geometry were tested without fuel injection to select the less flow-disturbing configuration. The nonreacting flowfields were also investigated by computation with a two-dimensional Navier–Stokes code. Using the selected strut, combustion and ignition tests were conducted. A pitot pressure and gas composition survey was carried out to deduce mixing and combustion efficiencies. It was found that mixing and combustion with a less flow-disturbing strut was considerably worse than those with a more flow-disturbing strut. Autoignition and forced ignition with plasma torches were tested for hydrogen. Ignition characteristics of parallel and perpendicular injection were quite different. The plasma igniters could successfully ignite both parallel and perpendicular fuel jets without a noticeable time delay between both sides of the strut.

Nomenclature

G = gap width of flow path
M = Mach number
m = mass flow rate
p = pressure
R = radius of strut leading edge
T = temperature
t = time
x = streamwise distance from step position
η = efficiency
θ = wedge half-angle of strut leading edge
ϕ = fuel equivalence ratio

Subscripts
a = air, vitiated air
c = combustion
LE = leading edge of strut
m = mixing
p = pilot fuel
s = strut
T = total fuel
t = stagnation condition
w = wall
0 = undisturbed upstream condition
$\parallel$ = parallel injection
$\perp$ = perpendicular injection

Received June 6, 1993; revision received July 11, 1994; accepted for publication Aug. 1, 1994.

*Head, Ramjet Aerodynamics Section, Ramjet Propulsion Research Division, Kakuda Research Center. Member AIAA.
†Senior Researcher, Ramjet Propulsion Research Division, Kakuda Research Center.
‡Researcher, Ramjet Performance Section, Ramjet Propulsion Research Division, Kakuda Research Center.
§Research and Development Center, Aerospace Division.
¶Engine Design Department, Research and Engineering Division, Aero-Engine and Space Operation.
**Senior Engineer, Research Institute.

Introduction

AMONG various performance parameters for scramjet combustors, ignition and mixing are the most important ones. In order to improve mixing, fuel injection struts have been installed in some subscale scramjet engines including the airframe integrated scramjet modules[1,2] and the dual mode engine.[1] A subscale scramjet engine now under fabrication[3] has been designed to be able to attach a fuel injection strut, too. In some of these engines, the struts were incorporated into the inlet for the final compression.[4,5] The struts, however, may cause several problems such as an increase of flow drag and severe heating. In our previous experiment,[6] the strut caused separation of the combustor wall boundary layers that propagated far upstream of the leading edge of the strut. In the present study, the effect of leading-edge geometry on the flowfield was examined both in experiment and computation.

Mixing and combustion performance with a less flow-disturbing strut were measured and compared with those of a more disturbing strut.[6] Upstream influence of combustion was also investigated.

Ignition characteristics of a scramjet combustor with a strut may be different from those without a strut. Huber et al.[7] reported that autoignition of fuel from struts occurred easier than that from the wall because the strut had a thinner boundary layer that resulted in a higher surface temperature than the wall. In the present study, autoignition and forced ignition of hydrogen from the strut was experimentally investigated. Small-size gas-cooled twin plasma torch igniters were developed for this test. The ignition characteristics of fuel from the strut were compared with those of fuel injected only from the walls.[8–11] Installation of struts would cause another problem relating to ignition. Since the struts divide the combustor into several flow paths, ignition of fuel jets in each flow path would occur independently. At least one igniter should be attached on each stream tube. Unless ignition in each path occurs almost simultaneously, a large transient pressure difference between two adjacent flow paths and severe side force on the strut would result. Such side force might cause structural damage on the strut, and could be one of the critical design issues.

In the present study, the time difference of the forced ignition in both sides of the strut was observed, too.

Experimental Apparatus

The experimental setup is illustrated in Fig. 1. A strut was inserted on the vertical plane of symmetry in a fuel injector block. Hydrogen at room temperature was injected from the strut and/or combustor walls. These configurations were basically the same as those used in our previous experiment.[6] However, for the present study, some modifications were made to install the plasma igniters with pilot fuel injection on the top wall and to allow fuel injection from the side walls. In ignition tests, the extension ducts of the combustor were removed to exclude ignition caused by interaction between the overexpanded test gas and atmospheric air.

Air Heater

Air was heated by a hydrogen vitiation heater[12] with oxygen replenishment. T_{ta} and p_{ta} of the vitiated air (or simply called as "air") were 800–2100 K and 1.0 MPa, respectively. T_{ta} was calculated assuming chemical equilibrium with the measured flow rates and pressure without considering incomplete combustion or heat loss. Air was then accelerated to Mach 2.5 by a two-dimensional nozzle with a 51- by 94.3-mm-rectangular exit cross section. At the nozzle exit, no unburnt hydrogen was detected and nonuniformity of water vapor concentration was less than 0.05 of the mean value.[12] Boundary-layer thickness based on pitot pressure measurement (99% of the freestream value) was about 10 mm for T_{ta} = 1000 K.

Isolator

The isolator was used to prevent propagation of precombustion shock as well as flow disturbance produced by the strut to the air heater nozzle. The isolator had a rectangular constant area cross section the same as the exit of the air heater nozzle and was 100 mm long.

Fuel Injector Block

Each flow path divided by the strut had the minimum cross section of 20 mm wide (gap width G) by 94.3 mm high. In the combustion performance tests, the side walls were flat and had a rearward-facing step at the end where the combustor began to diverge. They had no injection orifice. For the ignition tests, these side walls were replaced by other ones, each of which had a rearward-facing step of 2.0 mm ($0.1G$) height at the same location with that on the strut, and four orifices for perpendicular fuel injection at sonic speed. The center of the orifices were 8.0 mm ($0.4G$) downstream of the step. Diameter of the orifices was 2.5 mm. The top wall for the combustion performance test was flat and had no injection orifice, while that for the ignition test was similar to the one used in our previous igniter test[10] in strutless combustors. There was a 2.0-mm high-rearward-facing step at the same axial location as that on the strut, three pilot fuel orifices, and one plasma torch port in each flow path (see Fig. 2). The pilot fuel injection orifices had 1.0 mm diam and were placed 35 mm upstream the step. The plasma torch was placed 12.5 mm upstream the step. The central pilot orifice was directly upstream of the plasma jet orifice. The bottom wall was flat and had no injection orifice.

Strut

The strut had an arrowhead cross section. Five models with different wedge half-angle and radius of the leading edge, struts A–E of Fig. 3, were tested without fuel injection to select a less flow disturbing one. Strut E was used in a previous experiment[6] and resulted in a large separated area. Therefore, struts A–D had a smaller value of half-angle and/or radius than strut E. The maximum thickness of struts was 11 mm, and there was a rearward-facing step of 2.0 mm ($0.1G$) height on each side. The step location was the origin of the streamwise coordinate x. Only struts A and E could inject fuel. They were made of oxygen-free copper and their leading edges were water-cooled. Struts B, C, and D were made of copper and not cooled.

Struts A and E had five perpendicular injection orifices on each side at x/G = 0.4, and four parallel injection orifices on the base plane. The diameter of orifices was 2.5 mm. The perpendicular and parallel injection orifices are arranged in a staggered pattern. The perpendicular orifices on the strut are also staggered with those on the side walls. Two hydrogen feed lines were used to change the proportion of flow rates of the main and pilot fuel, the strut and wall injection, or the perpendicular and parallel jets, independently.

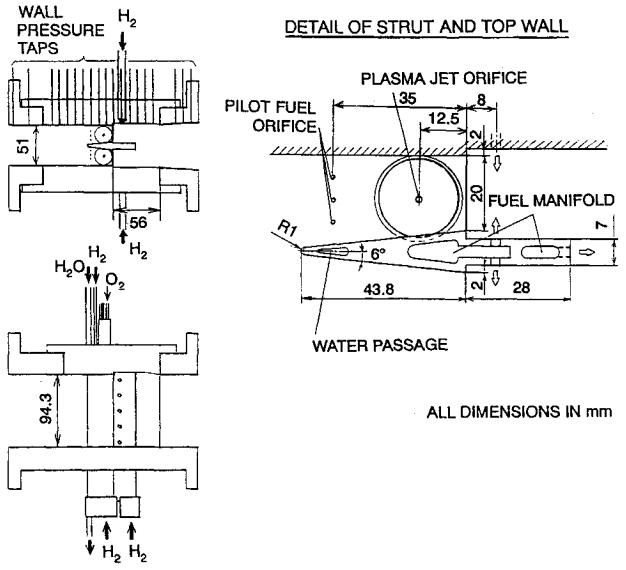

Fig. 2 Fuel injector block, strut, and plasma torch for ignition test.

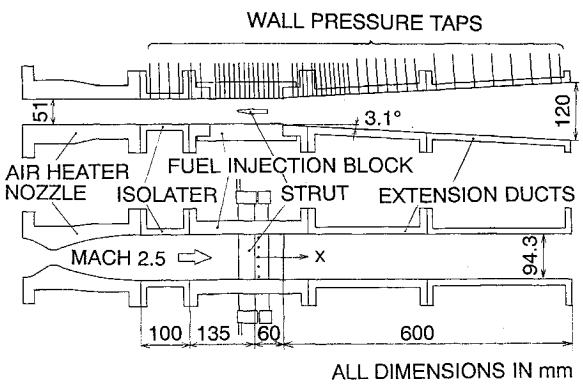

Fig. 1 Experimental apparatus for combustion performance test.

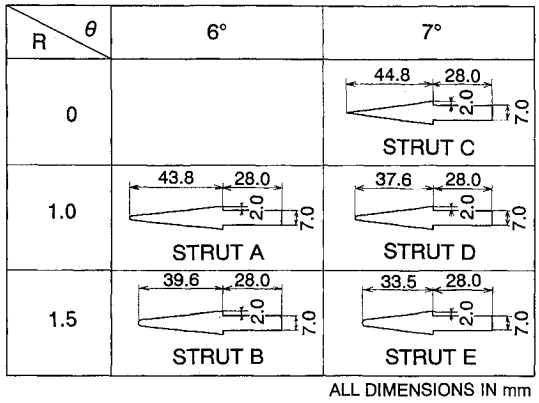

Fig. 3 Strut models.

Table 1 Plasma igniters for scramjet combustor

Authors	Diameter, mm	Length, mm	Feedstock	Power, kW	Coolant
Kimura[14]	86	193	H_2, N_2, Ar	2.8–5.7	Water
Northam[15]	50	50	Ar, Ar/H_2	1.5–3.4	Water
Wagner[16]	38	38	Ar/H_2	0.6–2.6	Heat sink
Sato[9,10]	35	163	O_2, Ar/H_2	3.2	Water
Stouffer[17]	45	94	Ar/H_2	0.5–1.1	Heat sink
Kudou[11]	23.5	75	O_2	1.0	Gas
Present	21	73	O_2, Air	1.0	Gas

Extension Ducts

The extension ducts were attached to the exit of the fuel injection block. The side walls of the ducts were diverging with a half-angle of 3.1 deg, while the top and bottom walls were parallel.

Plasma Torch Igniter

Twin plasma torch igniters were developed for the present study. Major specifications of the torch are summarized in Table 1 with other plasma torches for supersonic combustion.[9-11,14-17] The present torch has the smallest diameter and is cooled by gas. Reduction of the diameter was required by the flow path gap width. The feedstock was oxygen and its flow rate was 10 l/min. Experimental[9-11] and theoretical[18] studies indicated that oxygen plasma was very effective to ignite hydrogen. The cooling gas was oxygen, too. It flowed in a spiral passage around the torch nozzle, and ejected into the combustor from holes around the plasma jet orifice. Electric power for each torch was 1.0 kW. Details of the present plasma torch were reported by Ohwaki et al.[19]

Measurements

There were many pressure taps of 1.0 mm diam on the combustor walls, but none on the strut. Wall pressure distribution was measured by two mechanical pressure scanners. Wall pressure taps were used to measure wall temperature by inserting chromel-alumel thermocouples. Flow rates of gases (except oxygen for plasma torch) were measured by calibrated sharp-edge orifice flow meters. The feedstock of the plasma torch was measured by a float flow meter.

In order to deduce mixing and combustion efficiencies, a water-cooled 10-point pitot pressure/gas sampling probe rake was attached at the combustor exit. By changing the transverse location of the rake from run to run, 70 pieces of data were obtained in the exit section. Gas samples were also taken from wall pressure taps around the exit. Dry gas composition of the sample gas was obtained by a gas chromatograph with a Molecular Sieve 5A column. The method to calculate cross-sectional distributions and efficiencies was described in Ref. 13.

Signals from pressure transducers and thermocouples were amplified by dc amplifiers, digitized by a 12-bit analog/digital convertor, and stored on memories in a personal computer. Using calibration data, pressure, temperature, and flow rate were calculated. End-to-end accuracy of this measurement system was estimated to be 0.5%.

Ignition was detected by changes in wall temperature and pressure near the fuel injector, as well as video monitors of the exit in both horizontal and vertical directions to confirm whether fuel from the strut and the side walls were both ignited or if only one of them was ignited.

Procedure

Typical experimental sequence was as follows. At first, valves of air and plasma feedstock were opened. Then the plasma torches were turned on, valves of hydrogen and oxygen for vitiation were opened, and a spark plug ignited the air heater. It took about 3.5 s to establish steady heated airstream. Then hydrogen for the supersonic combustor was injected and measurement was conducted. About 7 s after the air heater was ignited, the plasma torches were turned off, then hydrogen and oxygen were shut off and, finally, air and plasma feedstock were shut down.

Computation

In order to clarify the effect of strut geometry on the flowfields, two-dimensional Navier–Stokes simulation was carried out with a fourth-order pointwise nonoscillatory scheme, which is called as the KRC scheme.[20] The most important feature of this scheme is that the numerical flux is defined as the pointwise value at the computational cell boundary, although the solution is pointwise. The implicit approximate factorization method is used for discretization in time. Chemical reaction was not specifically considered in the present calculation, but the value of 1.3 was used for the ratio of specific heats to calculate the flowfield of the vitiated air at $T_{t\infty}$ = 1000 K. The turbulence model used was the Baldwin–Lomax model.[21] Computational grids were 600 by 100. It took 10,000 steps to reach the steady-state solution for flow without major separation, and 100,000 steps with large separation bubbles.

Results and Discussion

Effect of Strut Configuration

Measured pressure distributions on the centerline of the side wall were shown in Fig. 4. For θ = 7 deg, struts C–E resulted in the same large-scale disturbance propagating upstream of their leading edges. For θ = 6 deg, strut B with R = 1.5 mm showed essentially the same pressure distribution as struts C–E, but strut A with 1.0 mm radius resulted in a much narrower disturbed region with a lower peak pressure than those of the other models.

Two typical flowfields, those with struts A and E, were computed. Predicted wall pressure distributions nondimensionalized by its undisturbed upstream value are compared with experimental results without injection in Fig. 5. Computed and experimental distributions for strut A show excellent agreement. Those for strut E agree well, too. These agreements indicate that the results of the computation sufficiently simulated the actual flowfields. Figure 6 shows calculated Mach number contours. The bow shock of strut A did not produce a large separation bubble, whereas strut E separated the wall boundary layer far upstream of its own leading edge.

The temporal evolution of the calculated flowfield suggests a development mechanism of such a large separated region. In the early stages of calculation, the bow shock from the leading edge reflected on the wall and impinged on the strut slightly upstream the step. This caused flow blockage and strengthened shock waves to separate the wall boundary layer. This separation went upstream and resulted in a large separation bubble. According to such processes, a relative position between the impingement point of the reflected bow shock and the step on the strut was a critical parameter to determining flowfield.

Combustion Performance

Combustion performance with strut A was measured and compared with those of strut E.[6] Fuel was injected only from

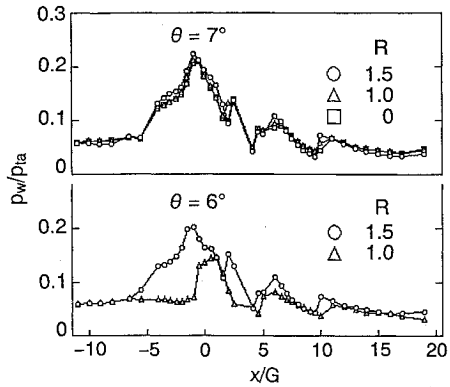

Fig. 4 Measured wall pressure distributions for struts with different leading-edge geometry without fuel injection.

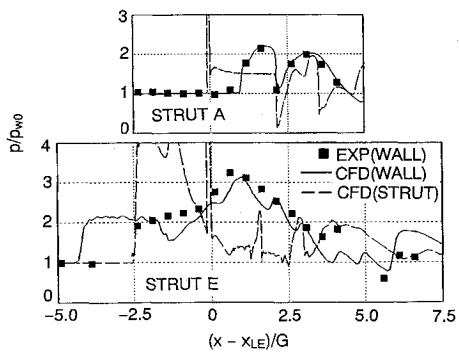

Fig. 5 Comparison of computed and measured wall pressure distributions for struts A and E.

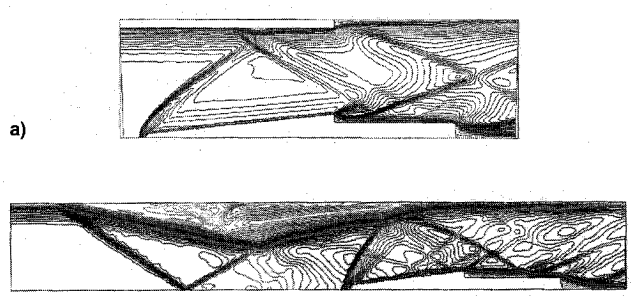

Fig. 6 Computed Mach number contours. Struts a) A and b) E.

the strut. Figure 7 shows wall pressure distributions for perpendicular and parallel injection into the airstream of T_{ta} = 2000 K. For perpendicular injection with $\phi_T = \phi_\perp = 0.5$, the wall pressure of strut A was consistently lower than that of strut E. For each strut with $\phi_T = \phi_\perp = 0.5$, the peak wall pressure of precombustion shock was only slightly higher than that of nonreacting flow. However, for $\phi_T = \phi_\perp = 0.6$, both distributions became the same and the precombustion shock went into the air heater nozzle. As in our previous experiment,[6] such combustion influence to upstream occurred as $\phi_\perp$ increased or T_{ta} decreased. However, $\phi_\parallel$ did not affect this phenomenon. Results of strut A for various combinations of perpendicular and parallel injections at several values of T_{ta} are summarized in Fig. 8. Solid symbols denote runs observed with upstream influence and the threshold is shown by a solid line. It is surprising that the threshold for strut A was almost the same as that of strut E, shown by a dashed line, despite a very significant difference in the nonreacting flowfield. Insensitivity of $\phi_\parallel$ on the threshold indicates that such upstream influence was governed by the extent of combustion within the fuel injector block.

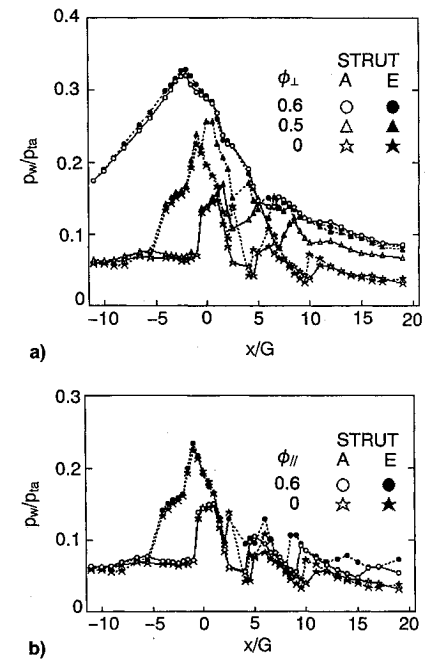

Fig. 7 Wall pressure distributions of combustion performance test (T_{ta} = 2000 K): a) perpendicular and b) parallel injections from strut.

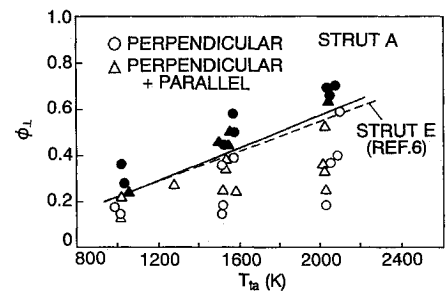

Fig. 8 Threshold of fuel flow rate for upstream influence by precombustion shock (solid symbols indicate runs with upstream influence).

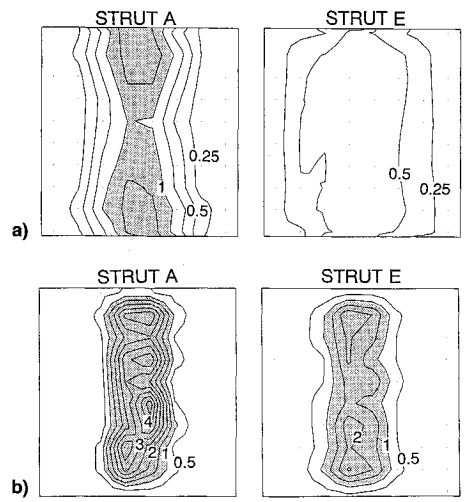

Fig. 9 Local fuel equivalence ratio distribution at x/G = 18 (T_{ta} = 1500 K, ϕ_T = 0.4): a) perpendicular and b) parallel injections.

Cross-sectional distributions of local equivalence ratio at x/G = 18 are shown in Fig. 9 for ϕ_T = 0.4 and T_{ta} = 1500 K. Fuel-rich regions were shaded. For both perpendicular and parallel injection, strut A resulted in much poorer mixing than strut E did. Perpendicularly injected fuel mixed much better than parallel injected fuel.

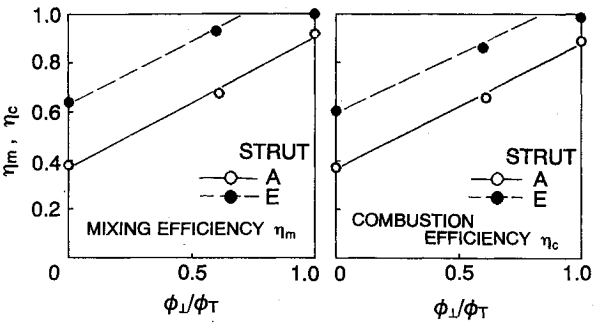

Fig. 10 Mixing and combustion efficiencies at x/G = 18 (T_{ta} = 1500 K, ϕ_T = 0.4).

Mixing and combustion efficiencies of struts A and E at x/G = 18 are compared in Fig. 10. Since ϕ_T was less than unity in this case, η_m was defined as the portion of fuel that could react without further mixing, while η_c was that actually reacted. For both struts A and E the difference between η_c and η_m was very small; thus, in the present experimental conditions, combustion was mixing-controlled. η_m and η_c for strut A were about 20% lower than those for strut E, except at $\phi_\perp/\phi_T$ = 1, where both efficiencies of strut E reached unity. Stronger shock waves produced by strut E more severely decelerated and disturbed the airstream than did those by strut A. The former also resulted in a lower dynamic pressure of airstream that improved the penetration of perpendicular jets. Thus, mixing was enhanced with strut E. From this result, determination of strut geometry requires a tradeoff of its effects on engine performances, including combustion efficiency, flow drag, inlet starting, isolator length, and wall heating.

Similar mixing enhancement by precombustion shock was observed in the strutless combustor.[13] The precombustion shock was produced by combustion and, therefore, its strength was determined as a result of an interaction. In the present case, the bow shock of the strut was nearly the same as or stronger than the precombustion shock for $\phi_\perp \leq 0.5$. Deceleration and disturbance of the airstream was mainly governed by the bow shock.

In Fig. 10, η_c and η_m of both struts almost linearly increased as $\phi_\perp/\phi_T$ increased, as suggested by Northam and Anderson.[2] These results confirm that heat release rate could be controlled by changing $\phi_\perp/\phi_T$.

Ignition Characteristics

Effects of vitiation on ignition and flameholding have been discussed by several authors.[18,22,23] Radicals produced in the vitiation heater would enhance ignition,[18,23] whereas water vapor would suppress it.[18] Therefore, vitiation heaters might not be suitable to determine the absolute value of the ignition temperature. However, relative effectiveness of igniter, and of fuel injection pattern and/or its direction to the ignition temperature may be investigated using the vitiated air. The ignition study of this article focused on these relative effects.

Autoignition

Test results of autoignition of fuel from the wall and/or strut injection orifices are shown in Fig. 11. When fuel was injected from all of the orifices, the ratios of $\phi_{w\perp}$, $\phi_{s\perp}$, and $\phi_{s\parallel}$ are 0.5, 0.3, and 0.2 of ϕ_T, respectively. The autoignition limit for fuel from both side walls of the strutless combustor[8] is shown by the dashed curve in the figure. The trend of the present ignition limit for fuel from all the orifices was qualitatively the same as the dashed curve, but the present ignition temperature was considerably lower than that of the strutless combustor. Flow deceleration by strut shock wave provided higher static temperature and pressure and lower airspeed favorable to autoignition. Thinner boundary layer on the strut resulting in a higher surface temperature may be another

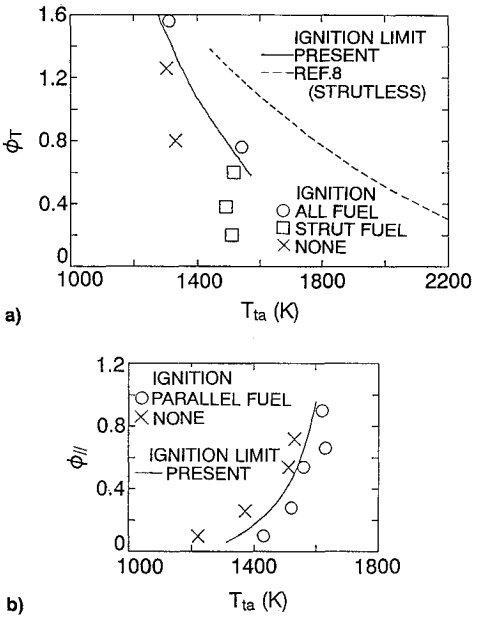

Fig. 11 Autoignition characteristics. Fuel from a) all of the injection orifices and b) from parallel injection orifices.

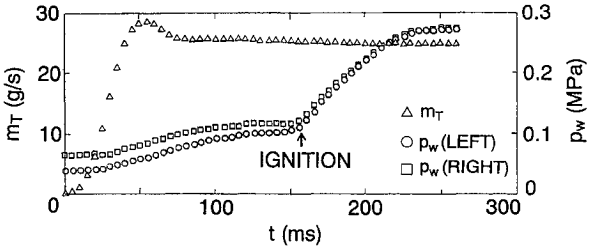

Fig. 12 Time history of wall pressures for ignition by plasma igniters (T_{ta} = 1073 K, ϕ_T = 0.42).

reason for this improvement. At low fuel flow rates, as expected from the latter reason, autoignition was observed only for fuel injected from the strut.

Fuel from the parallel injection orifices on the strut had a qualitatively different ignition limit curve as shown in Fig. 11b. Ignition became difficult as $\phi_\parallel$ increased. When fuel was injected perpendicularly, the recirculation region ahead of the fuel jet played an important role in the ignition. An increase of $\phi_\perp$ enlarged this region and resulted in lower ignition temperatures.[7,8] For parallel injection, however, the size of the recirculation region was determined by the dimensions of the strut base and was scarcely affected by $\phi_\parallel$, the fuel flow rate. Higher $\phi_\parallel$ would reduce the residual time of the fuel-air mixture in the base region and result in higher ignition temperatures. Such a tendency is consistent with results of ignition delay measurements for coaxial hydrogen jets in subsonic[24,25] or supersonic[25-27] airstreams. Since $\phi_{s\parallel}/\phi_T$ was 0.2, autoignition of the strut fuel in Fig. 11a corresponds to that of the parallel injection fuel.

Plasma Torch Ignition

The ignition time difference between two flow paths separated by the strut was first investigated with fuel from all the orifices. Figure 12 shows typical wall pressure histories of every 5 ms at the side wall steps. No significant time difference in pressure rise was observed. These results confirmed that the present igniter could suitably ignite fuel in both flow paths without a noticeable time difference.

The effect of ϕ_p on the ignition limit was tested for fuel from all the orifices, and that from parallel injection orifices on the strut. Since the ignition limit of perpendicular fuel jets

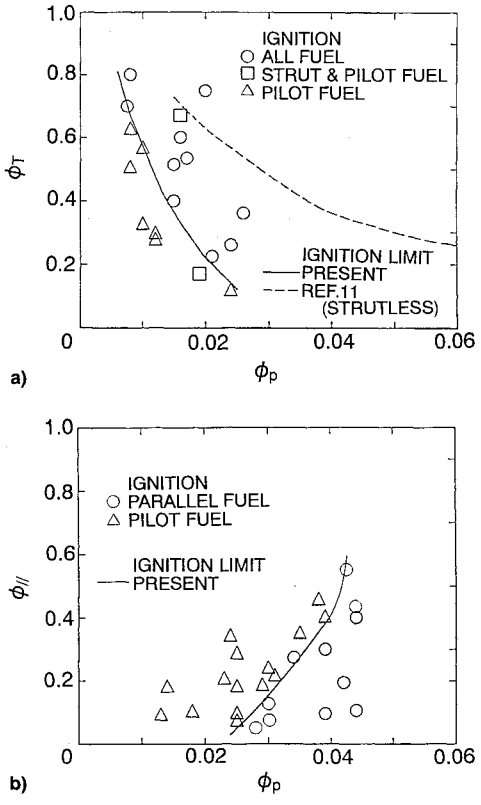

Fig. 13 Effect of pilot fuel flow rate on plasma torch ignition limit (T_{ta} = 1000 ± 50 K). Fuel from a) all the injection orifices and b) from parallel injection orifices.

by the plasma torch with pilot fuel changed little with T_{ta},[10] it was held constant at 1000 K. The present ignition limits were shown by a solid line on the ϕ_p-ϕ_T plane in Fig. 13. Note that in either case of fuel injection, fuel could not be ignited by the plasma torch without pilot injection. In the case using all of the orifices, ϕ_T of ignition limit decreased as ϕ_p increased. This is similar to the results[11] of the strutless combustors with perpendicular injection. In contrast, the ϕ_p required to ignite parallel jets increased as $\phi_{||}$ increased. Comparing with the autoignition results shown in Fig. 11b, we find that these forced ignition results are important, because they indicate that the increase of ϕ_p easily extends the ignition limit of fuel in scramjet combustors.

Conclusions

Flowfield and combustion/ignition characteristics of a supersonic combustor with a fuel injection strut were experimentally and computationally investigated. The following conclusions were obtained:

1) Nonreacting flowfield was sensitive to the leading-edge geometry of the strut. The relative position between the reflected bow shock wave impingement and the rearward step on the strut was a critical parameter.

2) Mixing and combustion efficiencies for a more disturbing strut were higher than those for a less disturbing strut due to more severe deceleration and disturbance of the airstream. In order to determine strut geometry, tradeoff of its influences on engine performances including combustion efficiency, flow drag, inlet starting, isolator length, and wall heating is required.

3) Mixing and combustion efficiencies of fuel injected from the struts were almost linearly increased with an increase of the flow rate ratio of the perpendicularly injected fuel to the total fuel.

4) The upstream influence of combustion was governed by the perpendicular injection flow rate, and the threshold fuel flow rate was not changed with the strut geometry.

5) Fuel from the strut ignited at a lower air temperature than that from the wall in both the autoignition and the forced ignition.

6) Autoignition and forced ignition of parallel fuel jets became easier for lower fuel flow rate, which is in contrast to the results of perpendicular injection. Ignition characteristics of the combined parallel/perpendicular jets were close to those of the latter.

7) The twin plasma torches with pilot injection could ignite perpendicular fuel jets of both flow paths without time lag, and they could also ignite parallel jets from the base of the strut.

8) Ignition limits with the plasma torch were extended by increasing pilot fuel flow rate.

Acknowledgments

This study was conducted as a part of the NAL-Nissan and NAL-IHI cooperative researches. The authors are grateful to N. Chinzei, K. Kudou, K. Itoh, and K. Tani of the National Aerospace Laboratory (NAL), T. Kuwahara and S. Miyamoto of Nissan Motor Co., and S. Yasu, K. Tsuchiya, and Y. Yonezawa of Ishikawajima-Harima Heavy Industries (IHI).

References

[1]Waltrup, P. J., Anderson, G. Y., and Stull, F. D., "Supersonic Combustion Ramjet (Scramjet) Engine Development in the United States," *Proceedings of the Third International Symposium on Air Breathing Engines* (Munich, Germany), 1974, pp. 835–861.

[2]Northam, G. B., and Anderson, G. Y., "Supersonic Combustion Ramjet Research at Langley," AIAA Paper 86-0159, Jan. 1986.

[3]Miyajima, H., Chinzei, N., Mitani, T., Wakamatsu, Y., and Maita, M., "Development Status of the NAL Ramjet Engine Test Facility and Sub-Scale Scramjet Engine," AIAA Paper 92-5094, Dec. 1992.

[4]Trexler, C. A., "Inlet Performance of the Integrated Langley Scramjet Module," AIAA Paper 75-1212, Sept. 1975.

[5]Tani, K., Kanda, T., Kudou, K., Murakami, A., Komuro, T., and Itoh, K., "Aerodynamic Performance of Scramjet Inlet Models with a Single Strut," AIAA Paper 93-0741, Jan. 1993.

[6]Komuro, T., et al., "Combustion Test and Thermal Analysis of Fuel Injection Struts of a Scramjet Combustor," *Proceedings of the 10th International Symposium on Air Breathing Engines* (Nottingham, England, UK), AIAA, Washington, DC, 1991, pp. 1228–1233.

[7]Huber, P. W., Schexnayder, C. J., and McClinton, C. R., "Criteria for Self-Ignition of Supersonic Hydrogen-Air Mixture," NASA TP-1457, Aug. 1979.

[8]Sato, Y., Sayama, M., Masuya, G., Komuro, T., Kudou, K., Murakami, A., Tani, K., and Chinzei, N., "Experimental Study on Autoignition in a Scramjet Combustor," *Journal of Propulsion and Power*, Vol. 7, No. 5, 1991, pp. 657, 658.

[9]Sato, Y., et al., "Effectiveness of Plasma Torches for Ignition and Flameholding in Scramjet," *Journal of Propulsion and Power*, Vol. 8, No. 4, 1992, pp. 883–889.

[10]Masuya, G., et al., "Some Governing Parameters of Plasma Torch Igniter/Flameholder in a Scramjet Combustor," *Journal of Propulsion and Power*, Vol. 9, No. 2, 1993, pp. 176–181.

[11]Kudou, K., Murakami, A., Komuro, T., Tani, K., Masuya, G., Sayama, M., and Ohwaki, K., "Forced Ignition by Reduced-Size Plasma Torch in a Scramjet Combustor," *Proceedings of the 35th Space Science and Technology Conference of Japan*, Japan Society for Aeronautical and Space Sciences, Nagaoka, Japan, 1991, pp. 387, 388 (in Japanese).

[12]Murakami, A., Komuro, T., Kudou, K., Masuya, G., and Chinzei, N., "An Air Heater for Scramjet Test," National Aerospace Lab., NAL TR-912, Tokyo, Japan, Sept. 1986 (in Japanese).

[13]Chinzei, N., Komuro, T., Kudou, K., Murakami, A., Tani, K., Masuya, G., and Wakamatsu, Y., "Effect of Injector Geometry on Scramjet Combustor Performance," *Journal of Propulsion and Power*, Vol. 9, No. 1, 1993, pp. 146–152.

[14]Kimura, I., Aoki, H., and Kato, M., "The Use of a Plasma Jet for Flame Stabilization and Promotion of Combustion in Supersonic Air Flows," *Combustion and Flame*, Vol. 42, No. 3, 1981, pp. 297–305.

[15]Northam, G. B., McClinton, C. R., Wagner, T. C., and O'Brien,

B. F., "Development and Evaluation of a Plasma Jet Flameholder for Scramjets," AIAA Paper 84-1408, June 1984.

[16]Wagner, T. C., O'Brien, B. F., Northam, G. B., and Eggers, J. M., "Plasma Torch Igniter for Scramjets," *Journal of Propulsion and Power*, Vol. 5, No. 4, 1989, pp. 548–554.

[17]Stouffer, S. D., O'Brien, B. F., and Roby, R. J., "Improved Plasma Torch for Ignition and Flameholding in Supersonic Combustion," AIAA Paper 89-2945, July 1989.

[18]Izumikawa, M., and Mitani, T., "Effects of Vitiated Air on Engine Tests in Wind Tunnel," *Proceedings of the 36th Space Science and Technology Conference of Japan*, Japan Society for Aeronautical and Space Sciences, Tokyo, Japan, 1992, pp. 279, 280 (in Japanese).

[19]Ohwaki, K., Yonezawa, Y., Tsuchiya, K., Kudou, K., Matumura, K., and Sonoda, H., "Development of Plasma Igniter for Scramjet Combustor," *Proceedings of the 33rd Conference on Aerospace Propulsion*, Japan Society for Aeronautical and Space Sciences, Naha, Japan, 1993, pp. 176–181 (in Japanese).

[20]Itoh, K., Tani, K., Tanno, H., Takahashi, M., Miyajima, H., and Asano, T., "A Numerical and Experimental Study of Free Piston Shock Tunnel," The 19th International Symposium on Shock Waves, Marseille, France, Paper 372, July 1993.

[21]Baldwin, B. S., and Lomax, H., "Thin Layer Approximation and Algebraic Model for Separated Turbulent Flows," AIAA Paper 78-257, Jan. 1978.

[22]Edelman, R., and Spadaccini, L. J., "Theoretical Effects of Vitiated Air Contamination on Ground Testing of Hypersonic Airbreathing Engines," *Journal of Spacecraft and Rockets*, Vol. 6, No. 12, 1969, pp. 1442–1447.

[23]Suttrop, F., "Comment on Experimental Study on Autoignition in a Scramjet Combustor," *Journal of Propulsion and Power*, Vol. 8, No. 6, 1992, pp. 1300–1302.

[24]Takeno, T., and Kotani, Y., "An Experimental Study on the Stability of Jet Diffusion Flame," *Acta Astronautica*, Vol. 2, Nos. 11 and 12, 1975, pp. 999–1008.

[25]Yoon, Y., Donbar, J. M., and Driskoll, J. F., "Blowout and Liftoff Limits of a Hydrogen Jet Flame in a Supersonic Heated, Coflowing Air Stream," AIAA Paper 93-0446, Jan. 1993.

[26]Suttrop, F., "Untersuchung über Zündhilfen für Überschall-Diffusionsflammen am Rande des Selbstzündungsbereichs," *Zeitschrift für Flugwissenschaften*, Band 19, Heft 4, 1971, pp. 163–168.

[27]Baev, V. K., and Yasakov, V. A., "Stability of a Diffusion Flame in Single and Mixed Jets," *Combustion, Explosion and Shock Waves*, Vol. 11, No. 2, pp. 143–154, *Fizika Goreniya i Vzryva*, Vol. 11, No. 2, 1975, pp. 163–178 (English Translation).